Molecular & Biochemical Parasitology 224 (2018) 1–5

Contents lists available at ScienceDirect

Molecular & Biochemical Parasitology

journal homepage: www.elsevier.com/locate/molbiopara

TbRRM1 knockdown produces abnormal cell morphology and apoptotic-like death in the bloodstream form of *T. brucei*

Analía G. Níttolo, Carolina P. Bañuelos, Juan I. Saborit, Valeria Tekiel, Daniel O. Sánchez, Gabriela V. Levy*

Instituto de Investigaciones Biotecnológicas, Universidad Nacional de San Martín (IIB-UNSAM), Consejo Nacional de Investigaciones Científicas y Técnicas (CONICET), 25 de Mayo y Francia, Gral. San Martín, 1650 Buenos Aires, Argentina

ARTICLE INFO

Keywords:
RNA binding protein
Cytokinesis
Annexin V
Mitochondrial membrane potential
Hypodiploidy
Flagellum detachment

ABSTRACT

TbRRM1, an SR-related protein, is involved in transcriptional and post-transcriptional gene expression regulation in procyclic *T. brucei*. In previous work, we found that TbRRM1 is essential and its depletion leads to cell cycle impairment, aberrant phenotypes and cell loss by apoptotic-like death. Here, we report the findings obtained after *TbRRM1* knockdown in bloodstream parasites. Depletion of TbRRM1 in this cell stage led also to growth arrest and cell loss by apoptosis-like death. However, microscopic analysis showed aberrant cell morphology with parasites displaying flagellum detachment and cytokinesis impairment after RNAi induction, suggesting that TbRRM1 could play different roles depending on parasite stage.

Trypanosoma brucei, a protozoan parasite belonging to the kinetoplastid group, causes Human African Trypanosomiasis (HAT) which is considered as one of the neglected tropical diseases. In spite of the number of new cases has dropped significantly over last years, HAT is still endemic in some regions of Africa [1]. According to the World Health Organization, many of the affected populations live in remote rural or unsafe areas where health systems are weak, hindering surveillance and therefore the diagnosis and treatment of cases.

Unlike most eukaryotic organisms, trypanosomes present some unusual biochemical features such as polycistronic transcription and the *trans*-splicing of a common sequence called *Spliced leader* to all mRNAs [2]. Because genes belonging to the same polycistronic transcription unit do not necessarily encode for functionally related proteins, it has long been thought that gene expression in kinetoplasts was regulated mainly at post-transcriptional level through the regulation of mRNA stability, translatability, or maturation [3]. These processes involve RNA binding proteins (RBPs) [4] which, albeit represented by only 80 genes in *T. brucei* [5], functional genomic approach leads to the identification of more than 300 proteins that could be involved at post-transcriptional level regulating the fate of mRNA molecules [6]. However, recent reports provided evidence suggesting an epigenetic regulation of gene expression controlled by histones and histone variant peaks [7] or by chromatin remodelers modifying the transcriptional machinery accessibility [8].

TbRRM1 (Tb927.2.4710), an SR-related RBP, was discovered twenty years ago [9]. This protein and the other two members of the SR-protein family (TSR1 and TSR1IP) are localized in nuclear speckles involving them to mRNA metabolism. Recently, TSR1 and TSR1IP have been implicated in the *cis* and *trans*-splicing processes and involved in the polyadenylation and stability of a subset of mRNAs regulated by them [10]. In contrast, the precise function of TbRRM1 protein remained elusive. Previous works have demonstrated that TbRRM1 is essential in the procyclic form (PCF) and, accordingly, *TbRRM1* knockdown leads to significant morphological changes and cell cycle impairment [11]. Recently, RIP-seq assays performed in PCF parasites allowed the identification of mRNAs associated to TbRRM1 thus suggesting that TbRRM1 could hold them into the nucleus avoiding their translation [12]. In addition, TbRRM1 was found to be associated to core histones regulating the chromatin structure since, after RNAi of TbRRM1, an increase of heterochromatin content was observed ([12] and data not shown). Moreover, our recent work indicates that TbRRM1 is involved in both facilitating transcription elongation of polycistronic transcription units and repressing the expression of monocistronic *SL-RNA* genes, two processes mediated by RNA Pol II (data not shown). Altogether, these reports suggest that TbRRM1 has several roles in PCF cells, including gene expression regulation at transcriptional and post-transcriptional levels.

In the present work, we evaluated the effect of *TbRRM1* knockdown

* Corresponding author.
E-mail addresses: anittolo@iib.unsam.edu.ar (A.G. Níttolo), cbanuelos@iib.unsam.edu.ar (C.P. Bañuelos), jsaborit@iib.unsam.edu.ar (J.I. Saborit), valet@iib.unsam.edu.ar (V. Tekiel), dsanchez@unsam.edu.ar (D.O. Sánchez), glevy@iib.unsam.edu.ar, gvlevy@gmail.com (G.V. Levy).

https://doi.org/10.1016/j.molbiopara.2018.07.006
Received 3 May 2018; Received in revised form 11 July 2018; Accepted 13 July 2018

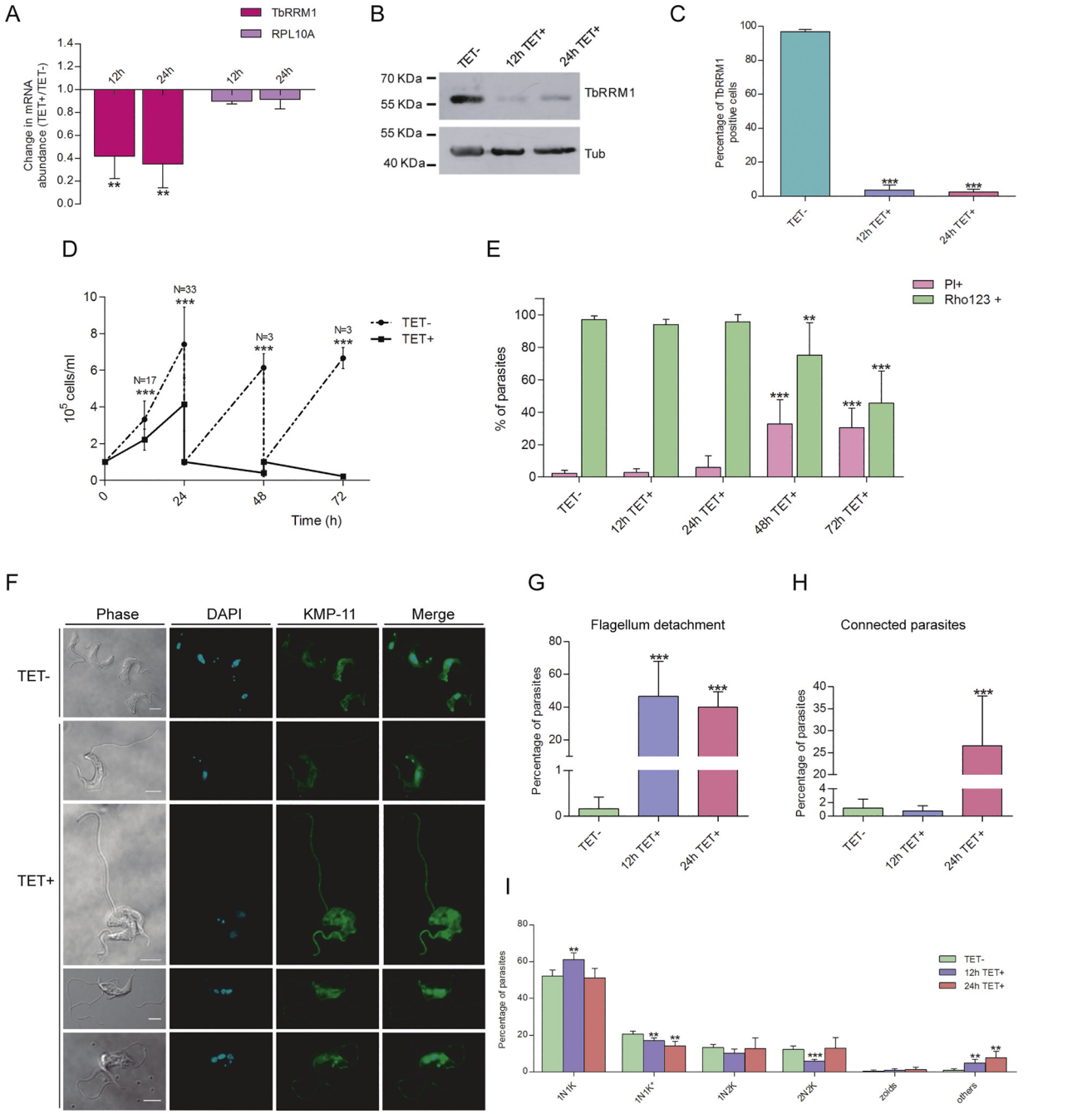

Fig. 1. RNAi validation assays and TbRRM1 depletion effects observed on parasite growth curve and cell morphology. (A) TbRRM1 mRNA levels after RNAi induction. Total RNA was extracted by TRIzol (Invitrogen) from TET− and TET+ cultures at 12 h or 24 h after *TbRRM1* knockdown. After RQ1 DNAse treatment (Promega), cDNA reaction was performed by SuperScript II enzyme (Invitrogen) and analyzed by RTqPCR. The values for TbRRM1 and for the ribosomal protein L10a (RPL10A, gene ID: Tb927.11.9710) were obtained by LinREG followed by REST software analysis and were normalized to 18S rRNA used as endogenous control. **(B)** Western blot of cultures at different times after TET addition were performed with anti-TbRRM1 antiserum followed by anti-mouse coupled to HRP antibody. Alpha-tubulin was used as loading control. **(C)** Quantification of parasites showing positive staining for TbRRM1 protein from more than 200 cells at each time point of three independent experiments. Indirect immunofluorescence (IIF) of parasites with anti-TbRRM1 antiserum followed by anti-mouse coupled to Alexa-488 antibody at different time points after RNAi induction. **(D)** Cell growth curve of parasites from TET− and TET+ populations. Cultures were initiated at 1×10^5 p/ml. Parasites were diluted daily at the initial concentration and were counted by Neubauer chamber. **(E)** Cell viability assay by Rho123 incorporation after RNAi induction. Samples were incubated 15 min with Rho123 (green bars) and PI (pink bars) and analyzed by FACS with a Partec CyFlow Space cytometer. **(F)** IIF with an anti-KMP11 antibody followed by incubation with anti-mouse Alexa-488 coupled antibody in parasites from induced and un-induced cultures was performed to visualize flagella (Scale bar: 3 μm). **(G)** Quantification of parasites showing flagellum detachment after *TbRRM1* knockdown. **(H)** Proportion of connected parasites found in TET− and TET+ cultures at different times after RNAi induction. **(I)** Nucleus (N) and kinetoplast (K) configuration assay by DAPI staining microscopy at different time points after TET addition. Each bar graph shows the mean ± SD of at least three independent biological replicates. Data from changes in mRNA abundance were analyzed by one sample Student *t*-test comparing to 1. Results in **G–I** were obtained from near 900 cells at each time point of at least three independent experiments. Unless otherwise indicated, data from other experiments were analyzed by two-tailed Student *t*-test comparing to TET- samples. $^{**}p < 0.01$, $^{***}p < 0.001$ (For interpretation of the references to colour in this figure legend, the reader is referred to the web version of this article).

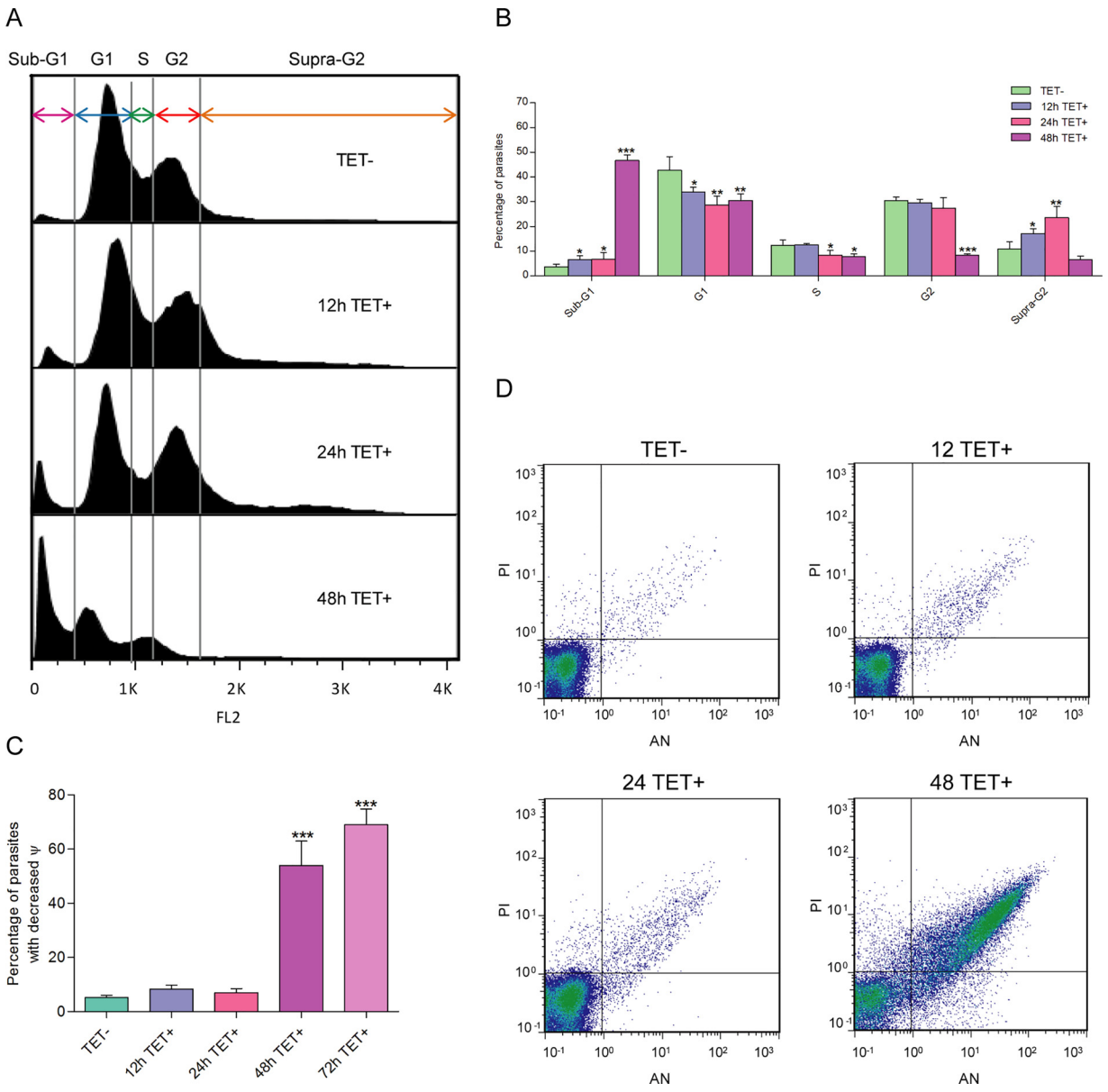

Fig. 2. TbRRM1 depletion leads to apoptotic cell death. (A) FACS profiles of PI-stained parasites after TbRRM1 depletion are shown as FL-2 histograms. TET− and TET+ cultures were washed in phosphate buffered saline (PBS)-10 mM glucose and resuspended in 0.1 M hypotonic phosphate buffer containing digitonin 6 μM and PI 10 μg/ml. Representative histograms of three independent biological replicates are shown. **(B)** Bars indicate the quantification of cell cycle distribution evaluated by FACS of parasites from TET− and TET+ cultures. **(C)** Proportion of Rho123 positive parasites showing lower levels of FL-1 intensity meaning a loss of mitochondrial membrane potential (ψ). **(D)** Dot blots showing the analysis of Annexin V and PI stained cell population by FACS after TbRRM1 depletion. Error bars represent the standard deviation around the mean of at least three independent experiments. Data were analyzed by two-tailed Student *t*-test compared to TET− samples. *$p < 0.05$, **$p < 0.01$, ***$p < 0.001$.

in the bloodstream form (BSF) of *T. brucei*. For that purpose, we transfected *T. brucei* Single Marker cell line with the p2T7^{TAblue}-Hygro vector (derived from [13]) containing a 424 bp fragment of the *TbRRM1* gene´s 5´UTR flanked by two opposite T7 promoters. *TbRRM1* knockdown in selected and cloned parasites was corroborated by measuring mRNA levels before and after Tetracycline (TET) addition (Fig. 1A). TbRRM1 protein depletion was evaluated by Western blot (Fig. 1B) and indirect immunofluorescence quantification showed that TbRRM1 reduction occurred from 12 h of TET addition in 96.4% of the parasite population (Fig. 1C). Cell growth curve analysis demonstrated that TbRRM1 is essential in BSF parasites, since after 12 h of TET addition, cell density dropped significantly comparing to un-induced cultures (Fig. 1D), suggesting that TbRRM1 protein plays a crucial role in BSF parasites as well as seen before in the procyclic stage [11]. The doubling cell time was calculated taking into account the cell density variation in culture and was found to be incremented from 8.4 h to 10.9 h or to 14.4 h after 12 or 24 h of culture, respectively. This result indicated that BSF cells presented delayed or altered cell cycle progression after depletion of TbRRM1.

To corroborate cell viability, parasites from TET− and TET+ cultures were incubated with Rhodamine123 (Rho123), a cell-permeant cationic green fluorescent dye that incorporates to mitochondria [14]. In parallel, cells were also incubated with propidium iodide (PI) to determine the percentage of dead parasites. FACS analysis showed a significant decrease in the number of parasites that incorporated Rho123 while the PI positive population increased after 48 h of RNAi induction (Fig. 1E). These results suggest that in spite of the affected parasite growth curve observed at 12 h of induction, parasites began to

die after 48 h, indicating some kind of quiescence or lethargy after TbRRM1 depletion.

Microscopic analysis of TbRRM1-depleted cells showed an uncommon proportion of parasites with abnormal morphologies (Fig. 1F), which included parasites displaying abnormal cell shape with flagellum detachment from the cell body after 12 h of *TbRRM1* knockdown (see Fig. 1G). This aberrant phenotype has been described earlier after knockdown of several flagellum attachment zone (FAZ) genes, leading to flagellar detachment [13], inhibition of basal body segregation [15] and altered cytokinesis [16]. Labelling of KMP11 by indirect immunofluorescence showed no differences in the basal body configuration before and after RNAi induction (data not shown). In addition, after 24 h of TET induction, we detected 26.6% of induced parasites connected by their posterior end, in contrast with only 1.2% observed in TET- cultures (Fig. 1H). This finding was similar to the incomplete division furrow ingression seen before, after depletion of the FAZ10 giant protein [17], suggesting that TbRRM1 absence produced also defects in cytokinesis.

Taking into account that the cell-growth arrest was observed from 12 h-on but parasite viability was compromised only after 48 h of TET addition, we characterized the cell cycle distribution after TbRRM1 depletion. For that purpose, cells were subjected to exhaustive microscopic analysis with DAPI staining to study the nucleus (N) and kinetoplast (K) configurations. In *T. brucei*, kinetoplast segregation precedes nuclear division, and therefore the NK configuration can help to elucidate cell cycle distribution [18,19]. Therefore, parasites presenting 1N1K are in the G1 phase of cell cycle, while those showing 1N2K or 2N2K belong to G2 or mitosis phase, respectively. Similarly, the kinetoplast morphology also contributes to evaluate the cell cycle distribution since parasites from the S-phase display an elongated kinetoplast (1N1K*) [18]. After 12 h of *TbRRM1* knockdown, an increment of 8.9% of the 1N1K parasite population and a concomitant decrease of the 1N1K* (from 20.7% to 17%) and 2N2K (from 12.2% to 5.8%) populations were observed (Fig. 1I). Nonetheless, this G1 cell accumulation effect was dissipated after 24 h of RNAi induction, as well as the decrease of parasites displaying 2N2K configuration, while 1N1K* parasite population continued to decline to 14.2%. In contrast to RNAi induction effects observed in PCF cells [11], the proportion of zoid parasites (0N1K) remained unaffected after TbRRM1 depletion in BSF cells. Additionally, an aberrant emerging group that included multinucleated cells, parasites with abnormal number of kinetoplasts and also those presenting misplaced NK configuration, was increased from 0.8 to 4.8% in induced cultures after 12 h of TET addition (***Others***, Fig. 1I). In all cases, results suggested alterations in mitotic or post-mitotic nuclear events after *TbRRM1* knockdown.

To further analyze the cell cycle distribution after TbRRM1 depletion, parasites from TET- and TET + cultures were permeabilized with digitonin, resuspended in hypotonic phosphate buffer and incubated with PI. FACS analysis showed that the G1 population decreased from 12 h of RNAi induction (Fig. 2A and B), in contrast to results obtained from NK configuration assay. In addition, parasites belonging to the S phase diminished from 12.4% to 8.4% after 24 h of TbRRM1 depletion. On the other hand, an increment of the sub-G1 cell proportion was observed from 12 h of TET addition. At 48 h of *TbRRM1* knockdown, this effect was markedly increased, according other cell cycle populations decreased, reaching the 49.3% of total cell population. These results suggest that TbRRM1 depletion led to parasite loss by an apoptotic-like death. Additionally, after 12 h of TET addition, the proportion of parasites with higher DNA content (supra G2 region) was increased probably due to the emergence of multinucleated parasites (Fig. 1F (third and fourth panel of TET + micrographs) and 1I (*others*)).

The apoptotic-like death after TbRRM1 depletion was corroborated by the Rho123 incorporation assay, which also allowed us to evaluate the mitochondrial membrane potential (ψ), a hallmark of apoptosis [20]. As shown in Fig. 2C the parasite population with impaired ψ increased after TbRRM1 depletion, reaching 54% and 69% after 48 and 72 h post-induction, respectively. This result suggested that parasites depleted of TbRRM1 die by an apoptotic-like mechanism. To further support this result, TbRRM1-RNAi parasites were induced or not with TET at different time points and co-incubated with AnnexinV (AN) and PI to detect the externalization of phosphatidylserine in apoptotic and dead cells, respectively. FACS results demonstrated that after 48 h of TET induction, both the AN + /PI- population indicative of a canonical early apoptotic state, and the AN + /PI + cell population, a sign of late apoptosis increased significantly (Fig. 2D). These data indicated that TbRRM1 depletion led to cell death by an apoptotic-like mechanism only after 48 h of TET addition.

Altogether, our results demonstrate that TbRRM1 protein is required for normal cell cycle progression in BSF parasites. In our previous work, we have shown that *TbRRM1* knockdown in PCF parasites leads to cell cycle progression impairment, abnormal cell morphology elongation compatible with the nozzle phenotype and parasite loss by an apoptotic-like mechanism [11]. In this work we observed 1N1K cell accumulation at 12 h post-RNAi induction, which could correspond to parasite differentiation to the non-replicative stumpy form (reviewed in [21]). However, results from FACS analysis indicated no cell cycle arrest after *TbRRM1* knockdown. Evaluation of cell cycle distribution by FACS is more precise than manually analyzed DAPI images and could explain the discrepancies obtained by both techniques. On the other hand, we also report here that TbRRM1 depletion produced aberrant cell morphology with parasites showing flagellum detachment and an increased number of joined parasites. These two events have not been described after TbRRM1 depletion in PCF cells, and suggest that TbRRM1 protein could be implicated in the gene expression regulation of some FAZ protein genes. Although TbRRM1 direct function remains to be elucidate, its depletion seems to trigger different events if comparing PCF and BSF parasites, suggesting that TbRRM1 could be associated to different mRNA molecules or could be modulating different regions at chromatin level in both cell stages.

Acknowledgments

Authors want to thank David Horn for kindly send us the p2T7$^{Ta\ Blue}$-Hygro vector and Juan Mucci for providing anti-KMP11 mouse serum. This work was supported by Agencia Nacional de Promoción Científica y Tecnológica, (ANPCyT, Argentina, PICT 2014-0879 to DOS and PICT 2014-0395 to GVL) and by the Consejo Nacional de Investigaciones Científicas y Técnicas (CONICET, Argentina). GVL, VT, and DOS are Career Investigators from CONICET.

References

[1] P. Buscher, G. Cecchi, V. Jamonneau, G. Priotto, Human African trypanosomiasis, Lancet 390 (10110) (2017) 2397–2409.
[2] T.N. Siegel, K. Gunasekera, G.A. Cross, T. Ochsenreiter, Gene expression in Trypanosoma brucei: lessons from high-throughput RNA sequencing, Trends Parasitol. 27 (10) (2011) 434–441.
[3] C.E. Clayton, Gene expression in Kinetoplastids, Curr. Opin. Microbiol. 32 (2016) 46–51.
[4] N.G. Kolev, E. Ullu, C. Tschudi, The emerging role of RNA-binding proteins in the life cycle of Trypanosoma brucei, Cell. Microbiol. 16 (4) (2014) 482–489.
[5] J.G. De Gaudenzi, G. Noe, V.A. Campo, A.C. Frasch, A. Cassola, Gene expression regulation in trypanosomatids, Essays Biochem. 51 (2011) 31–46.
[6] E.D. Erben, A. Fadda, S. Lueong, J.D. Hoheisel, C. Clayton, A genome-wide tethering screen reveals novel potential post-transcriptional regulators in Trypanosoma brucei, PLoS Pathog. 10 (6) (2014) e1004178.
[7] T.N. Siegel, D.R. Hekstra, L.E. Kemp, L.M. Figueiredo, J.E. Lowell, D. Fenyo, X. Wang, S. Dewell, G.A. Cross, Four histone variants mark the boundaries of polycistronic transcription units in Trypanosoma brucei, Gene Dev. 23 (9) (2009) 1063–1076.
[8] T.M. Stanne, M. Kushwaha, M. Wand, J.E. Taylor, G. Rudenko, TbISWI regulates multiple polymerase I (Pol I)-transcribed loci and is present at Pol II transcription boundaries in Trypanosoma brucei, Eukaryot. Cell 10 (7) (2011) 964–976.
[9] I.D. Manger, J.C. Boothroyd, Identification of a nuclear protein in Trypanosoma brucei with homology to RNA-binding proteins from cis-splicing systems, Mol. Biochem. Parasitol. 97 (1–2) (1998) 1–11.
[10] S.K. Gupta, V. Chikne, D. Eliaz, I.D. Tkacz, I. Naboishchikov, S. Carmi, H. Waldman

Ben-Asher, S. Michaeli, Two splicing factors carrying serine-arginine motifs, TSR1 and TSR1IP, regulate splicing, mRNA stability, and rRNA processing in Trypanosoma brucei, RNA Biol. 11 (6) (2014) 715–731.
[11] G.V. Levy, C.P. Banuelos, A.G. Nittolo, G.E. Ortiz, N. Mendiondo, G. Moretti, V.S. Tekiel, D.O. Sanchez, Depletion of the SR-related protein TbRRM1 leads to cell cycle arrest and apoptosis-like death in Trypanosoma brucei, PLoS One 10 (8) (2015) e0136070.
[12] A. Naguleswaran, K. Gunasekera, B. Schimanski, M. Heller, A. Hemphill, T. Ochsenreiter, I. Roditi, Trypanosoma brucei RRM1 is a nuclear RNA-binding protein and modulator of chromatin structure, mBio 6 (2) (2015) e00114.
[13] D.J. LaCount, B. Barrett, J.E. Donelson, Trypanosoma brucei FLA1 is required for flagellum attachment and cytokinesis, J. Biol. Chem. 277 (20) (2002) 17580–17588.
[14] A.A. Divo, C.L. Patton, A.C. Sartorelli, Evaluation of rhodamine 123 as a probe for monitoring mitochondrial function in Trypanosoma brucei spp, J. Eukaryot. Microbiol. 40 (3) (1993) 329–335.
[15] Q. Zhou, B. Liu, Y. Sun, C.Y. He, A coiled-coil- and C2-domain-containing protein is required for FAZ assembly and cell morphology in Trypanosoma brucei, J. Cell Sci. 124 (Pt. 22) (2011) 3848–3858.
[16] Q. Zhou, H. Hu, C.Y. He, Z. Li, Assembly and maintenance of the flagellum attachment zone filament in Trypanosoma brucei, J. Cell Sci. 128 (13) (2015) 2361–2372.
[17] B.P. Moreira, C.K. Fonseca, T.C. Hammarton, M.M. Baqui, Giant FAZ10 is required for flagellum attachment zone stabilization and furrow positioning in Trypanosoma brucei, J. Cell Sci. 130 (6) (2017) 1179–1193.
[18] T.N. Siegel, D.R. Hekstra, G.A. Cross, Analysis of the Trypanosoma brucei cell cycle by quantitative DAPI imaging, Mol. Biochem. Parasitol. 160 (2) (2008) 171–174.
[19] R. Woodward, K. Gull, Timing of nuclear and kinetoplast DNA replication and early morphological events in the cell cycle of Trypanosoma brucei, J. Cell Sci. 95 (Pt. 1) (1990) 49–57.
[20] E. Gottlieb, S.M. Armour, M.H. Harris, C.B. Thompson, Mitochondrial membrane potential regulates matrix configuration and cytochrome c release during apoptosis, Cell Death Differ. 10 (6) (2003) 709–717.
[21] E. Silvester, K.R. McWilliam, K.R. Matthews, The cytological events and molecular control of life cycle development of Trypanosoma brucei in the mammalian bloodstream, Pathogens 6 (3) (2017).